1990

Status Report on Polyalkylene Glycol Lubricants For Use With HFC-134A In Refrigeration Compressors

S. G. Sundaresan
Copeland Corp.

IMPACT OF THE CAPILLARY TUBE AND CONDENSER MODELLING APPROACH ON THE PERFORMANCE OF A DYNAMIC SIMULATION PROGRAM FOR DOMESTIC REFRIGERATORS

C. Melo (*), R.T.S. Ferreira (*), R.H. Pereira (**),A.L.M. Aranda (**)

(*) Department of Mechanical Engineering
Federal University of Santa Catarina
P.O. Box 476
88049 - Florianópolis - SC - Brazil

(**) Empresa Brasileira de Compressores S/A
Application Engineering
P.O. Box 476
89200 - Joinville - SC - Brazil

ABSTRACT

The objective of this work is to assess the sensibility of a computer simulation program, employed to analyse the transient behaviour of domestic refrigerators, to the adopted capillary tube and condenser mathematical modelling approach. Although all the comparisons, presented in this work, are related to a specific computer program, it is believed that, at least in a qualitative way, they are also valid for most of the computer simulation programs of vapor compression refrigerating systems, available in the open literature.

NOMENCLATURE

A	area, m^2
C	thermal capacity, kJ/K
Cp	specific heat, J/kgK
D	diameter, m
Dh	hidraulic diameter, m
e	fin thickness, m
f	friction factor
G	mass velocity based on tube cross-sectional area, kg/sm^2
H	stagnation enthalpy, kJ/kg
h	specific enthalpy, kJ/kg
hc	conv. heat transfer coef., W/m^2K
j	Colburn factor ($hcPr^{2/3}/QCp$)
K	entrance loss factor
k	thermal conductivity, W/mK
L	length, m
ℓ	distance between adjacent fins, m
M	mass, kg
$\dot{m}$	mass flow rate, kg/s
Nu	Nusselt number (hcD/k)
P	pressure, N/m^2
Pr	Prandtl number ($\mu Cp/k$)
Q	mass velocity in the coil where the minimum area occurs, kg/sm^2
R	thermal resistance, K/kW
Re	Reynolds number ($4Q/\pi D\mu$)
St	Stanton number (hc/QCp)
T	temperature, K
t	time, s
V	volume, m^3
v	specific volume, m^3/kg
x	vapor quality
Xa	transverse tube spacing, m
Xb	longitudinal tube spacing, m
y	fin height, m
Z	compressibility factor
β	constant
ΔT	temperature drop across condensate film, K
λ	latent heat, J/kg
μ	absolute viscosity, kg/ms
ρ	density, kg/m^3
σ	ratio of minimum flow area to frontal area

Subscripts

a	air
i	inlet, inside
f	fin
ℓ	liquid
o	outlet, outside
t	two-phase flow
v	vapor
w	wall
1	superheated region
2	saturated vapour region
3	saturated liquid region
4	subcooled region
∞	surroundings
*	previous time step

1. INTRODUCTION

For decades the only available technique to ascertain the performance of domestic refrigerators was to perform experimental tests, according to some specific standard, as for example the one presented in reference [1]. Such tests require, normally, a time period of, approximately, 24 hours, considering both the test period and the necessary time for the environmental test chamber to reach the initial steady state conditions. Nowadays the need for energy conservation and mainly, the need to replace CFC 12, in refrigeration systems, increased the required number of tests to such a level that most of the application laboratories are not able to manage. One way to speed up such procedure is to employ computational techniques to numerically simulate the refrigerator performance.

Particularly, in domestic refrigerators, which, normally, are thermostatic controlled, steady state conditions are rarely attained. According to this a numerical model for this kind of application should have transient characteristics. Unfortunately, most of the dynamic simulation models, available in the open literature, are directed towards heat pump simulation [2,3]. Within this context, it becomes necessary to develop a dynamic simulation computer program, specific to domestic refrigerators. The preliminary results of one of those programs, called REFSIM, were presented at the last Purdue Conference, by Melo et al.[4].

The main purpose of this work is to show how the condenser model and, consequently, the overall performance of the REFSIM program is affected by the approach adopted to evaluate the convective heat exchanges, both in the air and in the refrigerant side. Besides that the effect of adopting a detailed or a simplified capillary tube model, is also assessed.

2. CONDENSER MODELLING

The condenser is being modelled by three control volumes. Thus, at the beginning of the operation cycle, only the superheated vapor control volume is employed. As soon as the condensation process starts, the model neglects the superheated flow regime and employs only the saturated vapor control volume. The remaining control volume is employed when some subcooled liquid is found in the condenser.

The assumption of disregarding the influence of the superheated flow region, when some liquid is formed in the condenser, is valid only for forced-draft condensers, of the type considered in this work, since experimental results show that this region occupies only 5-10% of the total coil volume. This assumption is, obviously, not valid for natural-draft condensers.

Each control volume is treated as a stirred tank, in which the conditions existing at the outlet of the tank are the same as the bulk conditions within the tank. Applying the conservation equations for mass and energy to the superheated control volume, yields:

$$d(M_1)/dt = \dot{m}_i - \dot{m}_o \tag{1}$$

$$d(M_1 h_1)/dt = \dot{m}_i h_i - \dot{m}_o h_o - (T_1 - T_{w1})/R_{i1} \tag{2}$$

$$d(C_{w1} T_{w1})/dt = (T_1 - T_{w1})/R_{i1} - (T_{w1} - T_\infty)/R_{o1} \tag{3}$$

Combining equations (1) and (2) and considering that $h_o = h_1$, gives:

$$d(h_1)/dt = \left[\dot{m}_i(h_i - h_1) - (T_1 - T_{w1})/R_{i1}\right]/M_1 \tag{4}$$

Numerical integration of equations (1) and (4) yields, respectively, the mass of refrigerant in condenser and the bulk enthalpy of refrigerant vapor at the next time step. The refrigerant temperature and compressibility factor are respectively, calculated, by equations obtained via the polynomial regression technique. The pressure at the next time step is then calculated by the following expression:

$$P = P_* \, (ZM_1T_1)/(Z_*M_{1*}T_{1*}) \tag{5}$$

The temperature of the condenser coil material is calculated, for the next time step, by numerical integration of equation (3).

Applying the conservation equations for mass and energy to the control volume, indicated in Figure 1, the equations for the saturated and subcooled flow regions are derived. It should be mentioned that the saturated or mixed region is the volume of the condenser which contains the superheated vapor and the saturated refrigerant. Thus,

$$d(M_{2-3})/dt = \dot{m}_i - \dot{m}_o \tag{6}$$

where

$$M_{2-3} = M_2 + M_3 \tag{7}$$

It should be noted that the mass flow rate of saturated liquid leaving the mixed region, is assumed to be equal to the mass flow rate at condenser outlet, since the liquid refrigerant can be considered as incompressible.

Combining equations (6) and (7), gives:

$$d(M_2)/dt = \dot{m}_i - \dot{m}_o - \dot{m}_\ell \tag{8}$$

Where $\dot{m}_\ell$ represents the rate of change of mass of liquid in the saturated region.

Applying the energy equation to the saturated region and replacing the refrigerant internal energy by the refrigerant enthalpy, in the transient term, yields:

$$d(M_2h_2)/dt + d(M_3h_3)/dt = \dot{m}_i h_i - \dot{m}_o h_3 - (T_2 - T_{w2})/R_{i2} \tag{9}$$

$$d(C_{w2}T_{w2})/dt = (T_2 - T_{w2})/R_{i2} - (T_{w2} - T_\infty)/R_{o2} \tag{10}$$

Combining equations (7) and (8) and considering the simplifications suggested by Dhar [5], gives:

$$\dot{m}_\ell = \left[\dot{m}_i(h_2 - h_i) + \dot{m}_o(h_3 - h_2) + (T_2 - T_{w2})/R_{i2}\right]/(h_2 - h_3) \tag{11}$$

Numerical integration of equations (6) and (11) yields, respectively, the total mass and the liquid refrigerant mass in condenser. The vapour refrigerant mass is then obtained from equation (7).

The pressure at the new time step is then calculated by the following equation:

$$P = P_*(V_{2*}M_2Z_2T_2)/(V_2M_{2*}Z_{2*}T_{2*}) \tag{12}$$

The variables T_2, h_2, h_3 and Z_2 are then calculated from property relations. The condenser wall temperature is calculated for the next time step by numerical integration of equation (10).

Applying the energy equation to the subcooled region, gives:

$$d(M_4h_4)/dt = \dot{m}_o h_3 - \dot{m}_o h_4 - (T_4 - T_{w4})/R_{i4} \tag{13}$$

$$d(C_{w4}T_{w4})/dt = (T_4 - T_{w4})/R_{i4} - (T_{w4} - T_\infty)/R_{o4} \tag{14}$$

Numerical integration of equation (13) gives the bulk enthalpy of the subcooled refrigerant. The bulk temperature is then calculated from property relations. Numerical integration of equation (14) gives the condenser wall temperature.

It should be noted that the volume of vapour in condenser as well as the thermal resistances, indicated in the previous equations, are dependent on the lengths L_2 and L_4, shown in Figure 1. Such parameters are reevaluated at each time step in order to update those variables. This updating process is performed, in the REFSIM program, according to the process suggested by Dhar [5].

In a previous work, Melo et al. [4], employed thermal resistances calculated in accordance to the equations presented by Domanski and Didion [6], and by Tandon et al. [7]. Those calculations were based on steady state conditions, and the resultant values were kept constant along the time, in spite of the transient characteristic of the program. Despite of the relative success of such procedure, when the system refrigerant charge or the test conditions or the dimensions of any component were altered, the referred thermal resistances needed to be reevaluated. Besides that there was always a need for a preliminary experimental test in order to obtain the steady state parameters required for such procedure. Therefore it was decided to implement specific routines, in the REFSIM program, in order to be able to evaluate the thermal resistances at each time step.

3. CONVECTIVE HEAT TRANSFER CORRELATIONS FOR THE CONDENSER

Several correlations are available in the open literature which can be used to calculate the convective heat transfer in the condenser. Next, the equations of most common use are presented and their impact on the refrigeration system simulation program REFSIM are discussed and analyzed.

3.1. Air Side Correlations

For the condenser air side, five correlations can be considered. The first equation, presented by Domanski and Didion [6], is given by:

$$Nu_a = 0.134\ Re_a^{0.681}\ Pr_a^{0.333}\ (\ell/y)^{0.2}\ (\ell/e)^{0.1134} \tag{15}$$

The second correlation has been derived from the work of Kays and London [10], considering a situation very close to the condenser under analysis,

$$St_a\ Pr_a^{0.667} = 0.187\ Re_a^{-0.416} \tag{16}$$

The third correlation tested in the program has been selected from the work of Gray and Webb [9]. Considering that the condenser under analysis has only two rows, this correlation can be reduced to:

$$j = 0.649\ Re_a^{-0.495}\ (XaXb)^{-0.502}\ (\ell/D_o)^{0.0312} \tag{17}$$

The fourth correlation to be considered is given by Trauger and Webb [10]. This equation is especially recommended for condensers with wavy fins and consists in the determination of a constant, which is based on the condenser geometrical dimensions, to be multiplied by Eq. (17).

Finally, the fifth equation is given by McQuiston [11]:

$$j = F\left[266.66(Re_a^{-0.6}\ \ 4XaXb\sigma/\pi DhD_o) + 1.33\right]10^{-3} \tag{18}$$

where the multiplication factor F is used to adjust the Colburn coefficient j to situations where the number of rows is different from four.

3.2. Refrigerant Side Correlations

Considering the regions of single-phase flow in the condenser, which are the superheatead and subcooled regions, the thermal resistance has been evaluated after calculating the convective heat transfer coefficient given by Dittus - Boelter correlation [6], and using the refrigerant properties in each one of the independent regions.

The predominant pattern in the two-phase flow region in a refrigeration system condenser is annular flow with liquid refrigerant flowing on the pipe wall and vapor refrigerant flowing in the core. Two correlations are traditonally used for this two-phase flow region. The first equation is given by Tandon et al. [7].

$$Nu = 0.084\ Pr_\ell^{0.333}(\lambda/Cp_\ell\Delta T)^{0.1667}\ Re_V^{0.67}\ ,\ Re_V > 3x10^4 \tag{19}$$

$$Nu = 23.1\ Pr_\ell^{0.333}(\lambda/Cp_\ell\Delta T)^{0.1667}\ Re_V^{0.125}\ ,\ Re_V < 3x10^4 \tag{20}$$

The second correlation is given by Traviss et al. [12].

$$Nu = (Pr_\ell Re_\ell^{0.9} F_1)/F_2 \tag{21}$$

where the parameters F_1 and F_2 are fully described in [12]

3.3. Comparative Analysis

The refrigeration system to be considered is indicated in Figure 2. It is basically composed by a reciprocating compressor, two forced-draft heat exchangers and an adiabatic capillary tube.

All the simulations have been performed using different combinations of the correlations for the inner and outer side of the condenser. The results of these simulations are discussed next. As all the outside correlations for the condenser depend upon the air conditions and its geometrical characteristics, they can be compared independently of the correlation being used for the refrigerant side of the heat exchanger. Therefore, plugging in the constant numerical values into the equations presented in section 3.1, the air side thermal resistances can be calculated. In doing so the values of 33.4, 67.8, 42.8, 21.9 and 36.8 W/mK, are then calculated by using the different correlations in the same order as presented above.

As it can be observed, the first [6] and fifth [11] correlations give very close results. Therefore only the last one will be used. Also one can see that the second correlation [8] furnishes extremely high values for the air side thermal resistance what gives rise in the simulation to very high condensing pressures, which are incompatible to experimental evidences. Thus, this equation is eliminated from the following analysis. Figure 3 shows the comparison for the evaporating and condensing numerical pressures, calculated using the correlations given by Gray and Webb [9], Trauger and Webb [10] and McQuiston [11], together with the experimental results. In Fig. 3a the equation given by Traviss et al. [12] has been used for the two-phase flow region while in Fig. 3b, for the same region, the correlation by Tandon et al. [7] has been employed. As it can be seen, the REFSIM program gives significantly different results for the pressures variation with time according to the correlation being used to calculate the convective heat transfer at the inner and outer sides of the condenser. In Fig. 3a one can observe that none of the correlations give a reasonable result for the discharge pressure along the time. By the other hand, it can be verified that, in Fig. 3b the use of the correlation given by Trauger and Webb [10] permits a very good agreement for the condensing pressure with the experimental results, especially after the first minute of operation.

It can be seen that the suction pressure is not affected by the use of any one of the correlations. This is so because the evaporator thermal resistances are calculated for the steady state condition and are kept constant along the time. In a future stage this type of analysis will also be performed for the evaporator.

It is evident from Figs. 3a and 3b that the substitution of the correlation furnished by Traviss et al. [12] by the one given by Tandon et al. [7], for the two-phase flow region, improves quite a bit the agreement between numerical and experimental results. Fig. 4 presents the variation of the two-phase flow thermal resistances with time calculated using both equations given by [7] and [12]. The air side thermal resistance in both cases were calculated using the correlation given by Trauger and Webb [10].

It is important to emphasize that the program REFSIM executes a dynamic simulation and so the mass flow rates at the entrance and at the exit of the two-phase flow region are different from one another especially at the beginning of the compressor start-up. Therefore it is necessary to decide which mass flow rate should be used to calculate the respective Reynolds number. Using the correlation given by Trauger and Webb [10] for the condenser refrigerant side one can get the results for the flow Reynolds number and the correspondent Nusselt number in the saturation region, as shown in Figs. 5 and 6, respectively. The mass flow rate in these Figures were calculated using the following equation:

$$\dot{m} = (1 - \beta)\, \dot{m}_i + \beta \dot{m}_o \qquad (22)$$

where β ranges from 0 to 1.

From Figs. 5 and 6, one can see that the Reynolds number and the Nusselt number, for the two-phase flow region, are highly dependent upon the adopted mass flow rate, especially in the first minute of the simulation. However, for the present analysis such variation does not promote any modification in the discharge pressure, as the condenser heat transfer, for the case under analysis, is dominated by the air side resistance. This observation cannot be generalized though.

4. CAPILLARY TUBE MODELLING

Melo et al. [4] used, with reasonable good results, a simplified model for the capillary tube, in an early stage of this work. However, this simplified model had to be replaced by a more refined one because it had been shown inadequate for different operating conditions of the refrigerator. Also the availability of more powerful computational resources permitted this improvement. This refined model will be described next and comparisons of the numerical results of the REFSIM program using each one of the models for the capillary tube will be presented.

4.1 - Pressure and Temperature Distributions in Capillary Tubes

The capillary tube shows a very complex working behavior, despite of being very simple in construction. Fig. 7 shows the refrigerant pressure and temperature profiles along a typical capillary tube. Just after entering the capillary tube, the refrigerant, in the subcooled state, shows a small pressure drop due mainly to the abrupt change in the cross section area. Considering the process as being adiabatic, from point B to point C the pressure decreases linearly while the temperature is kept constant. Point C is the flash point where the flow reaches saturated conditions. From this point on, the pressure reduces more rapidly than in the previous section and the temperature shows a correspondent decrement. The dashed lines in Fig. 7 indicate different paths which can occur in a capillary tube depending upon its geometrical and its working conditions. Between points C and D, experimental measurements indicate the presence of liquid refrigerant. The pressure drop indicated between points D and E is due to the sonic conditions being reached by the flow at the exit of the capillary tube. This situation, also called critical condition, corresponds to the point where the refrigerant entropy reaches its maximum value. The flow through the capillary tube cannot be further accelerated when the choked conditions are established. The pressure in this situation is called critical pressure and must be conveniently calculated in order to correctly determine the mass flow rate through the tube.

4.2 - Numerical Model

The main assumptions involved in establishing the numerical model are the following: i) the capillary tube is a straight, horizontal, constant area tube, ii) flow in the capillary tube is one-dimensional, homogeneous and adiabatic, iii) the refrigerant fluid is free of oil and iv) metastable flow phenomena are neglected.

For the liquid region in the capillary tube, according to Fig. 7, the pressure difference between points A and C can be calculated by:

$$P_A - P_C = (1 + K + f_\ell L_\ell/D)G^2/2\rho_\ell \tag{23}$$

where the pressures P_A and P_C correspond, respectively to the condensing pressure and the saturated pressure at the temperature of the subcooled liquid. The friction factor for the liquid region is calculated according to reference [8].

For the two-phase flow region, the flow follows a Fanno line. Applying the energy equation for a general Fanno flow between points C and D and expressing the fluid enthalpy and density in this saturated region as a function of the local vapor quality, x, yields:

$$x = \left\{h_{\ell v} - G^2 v_\ell v_{\ell v} + \left[(h_{\ell v} + G^2 v_{\ell v} v_\ell)^2 - 2(G^2 v_{\ell v}^2)(h_\ell + G^2 v_\ell^2/2 - H)\right]^{0.5}\right\}/G^2 v_{\ell v}^2 \tag{24}$$

Applying the momentum conservation equation to a fluid element of length dℓ in the two-phase flow region, and integrating between points C and D one gets:

$$\bar{f}_t L_t/D = 2\ln(\rho_D/\rho_C) - (2\int_C^D \rho dP)/G^2 \tag{25}$$

where the average friction factor in the two-phase flow region, $\bar{f}_t$, according to Erth [13], can be calculated by:

$$\bar{f}_t = 3.1\, Re_i^{-0.5} \exp\left[(1-x_i^{0.5})/2.4\right] \tag{26}$$

The integral in Eq. (25) is numerically calculated by the Romberg's process, while the refrigerant properties are evaluated through polynomial equations. In order to determine whether the flow is critical, the local refrigerant entropy values are calculated using Eq. (24) and the fluid properties at saturation. Using a numerical procedure, the pressure, for which the entropy is maximum, can be easily determined. This choked pressure is then compared to the evaporating pressure (point E), and the bigger value will be used in Eq. (25) as P_D.

Starting from this model, one can build a computational structure to be incorporated in a general simulation program for refrigeration systems in order to calculate the mass flow rate through the capillary tube, as a function of the geometrical parameters D and L, and the operating conditions. This solving process has to be iterative though, once the mass flow rate depends upon the friction factors and the dynamic pressure at the entrance of the capillary tube, which by their turn are dependent on the mass flow rate. The best iterative process, which results in a minimum CPU time, consists in firstly estimating the mass flow rate and calculating the physical lengths L_ℓ and L_t. The overall length of the capillary tube has to be equal to the sum of L_ℓ (liquid region) and L_t(two-phase region). The mass flow rate initially guessed is then corrected and the process continues until the convergence is reached.

4.3 - Comparative Analysis

In this section the numerical results of the REFSIM program using the simplified model for the capillary tube [4] and the present model are compared and discussed. Fig. 8 shows that the pressure-time history calculated by REFSIM is sensibly improved when the refined model for the capillary tube is used. One can also note that the simplified model, for the case under analysis, produces the interruption of the simulation 3.2 minutes after the compressor start-up. This interruption is mainly due to the fact that the possibility for the choked flow in the simplified model was not considered. As it can be observed from Fig. 9, the critical pressure, after 24s from the compressor start-up is consistently greater than the evaporating pressure. Therefore, the simplified version model calculates a greater mass flow rate in the capillary tube, which empties the condenser and stops the program, as shown in Figs. 10 and 11.

5. CONCLUSIONS

The present work focused different aspects related to the condenser and capillary tube models. The influence of the different modelling approaches for those components in a domestic refrigerator simulation program was performed using REFSIM [4], which was developed for the dynamic analysis of small refrigerating systems.

It is evident that the use of different heat transfer correlations available in the open literature for both sides of the condenser has a significant influence on the predicted performance of the system. The identification of the correct heat transfer correlations to be used in the simulation program is on the same level of importance as the detailed description of the whole condenser. It does not seem reasonable to move towards a more sophisticated differential model for the condenser or any other component with all the difficulties involved in void fraction models and other complexities, if the simple convective heat transfer coefficients cannot be reliably calculated. By other hand, the adiabatic capillary tube model needs a more detailed description even if an integral analysis is used.

Besides those conclusions were related to a specific simulation code, they can be applied to the great majority of the existing simulation programs.

6. REFERENCES

[01] Standard ISO-24, Performance of Household Refrigerating Appliances - Refrigerators and Freezers, 1986.

[02] Chi J. and Didion, D., A Simulation of the Transient Performance of a Heat Pump, International Journal of Refrigeration, Vol. 5, no. 3, pp. 176-184, 1982.

[03] Yasuda, H., Touber S. and Machielsen , C.H.M., Simulation Model of a Vapor Compression Refrigeration System, ASHRAE Transactions, Vol. 89, part 2A, no. 2787, pp. 408-425, 1983.

[04] Melo, C., Ferreira, R.T.S., Pereira, R.H. and Negrão, C.O.R., Dynamic Behaviour of a Vapor Compression Refrigerator: A Theoretical and Experimental Analysis, Proc. of the 1988 I.I.R. Meeting, Commissions B1, B2, E1, E2, Purdue University, USA, pp. 141-149, 1988.

[05] Dhar, M., Transient Analysis of Refrigeration System, Ph. D. Thesis, Purdue University, 1978.

[06] Domanski, P. and Didion, D., Computer Modeling of the Vapour Compression Cycle with Constant Flow Area Expansion Device, NBS Building Science 155, National Bureau of Standards, Washington - DC, USA, 1983.

[07] Tandon, T.N., Varma, H.K., Gupta, C.P., An Experimental Investigation of Forced Convection Condensation During Annular Flow Inside a Horizontal Tube, ASHRAE Transactions, Part 1A, pp. 343-355, 1985.

[08] Kays, W.M. and London, A.L., Compact Heat Exchangers, 3rd edition, Mc Graw-Hill Book Co., New York, 1984.

[09] Gray, D.L. and Webb, R.L., Heat Transfer and Friction Correlations for Plate Finned-Tube Heat Exchangers Having Plain Fins, Proc. of 8th Int. Heat Transfer Conference, San Francisco, 1986.

[10] Trauger, P. and Webb, R.L., A Correlation for the Air Side Heat Transfer Coefficient for a Wavy Fin (to be published).

[11] McQuiston, F.C., Finned Tube Heat Exchangers: State of the Art for the Air Side, ASHRAE Transactions, Vol. 87, Part. 1, pp. 1077-1085, 1981.

[12] Traviss, D.P., Rohsenow, W.M., and Baron, A.B., Forced Convection Condensation Inside Tubes: A Heat Transfer Equation for Condenser Design, ASHRAE Transactions, Vol. 79 Part 1, pp. 157-165, 1973.

[13] Erth, R.A., Two-Phase Flow in Refrigeration Capillary Tubes: Analysis and Prediction, Ph.D. Thesis, Purdue University, USA, 1970.

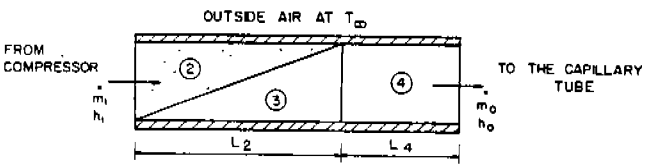

Fig . 1 - Schematic lay out of the condenser saturated and subcooled regions

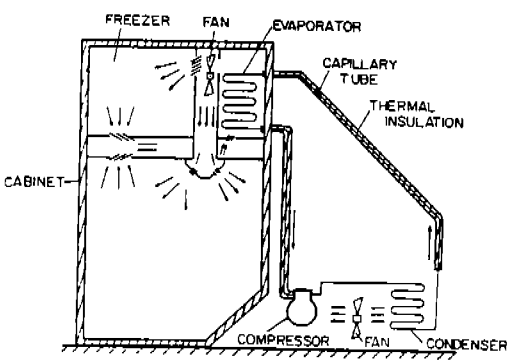

Fig . 2 - Domestic refrigerator under analysis

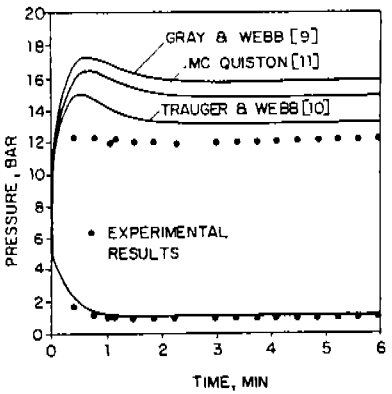

a) Traviss et al.[12] correlation

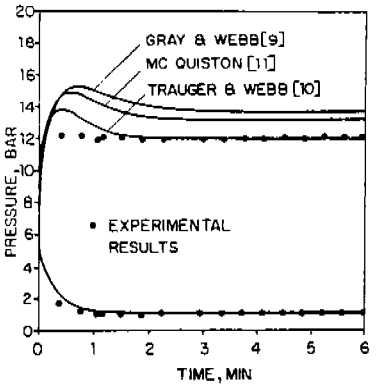

b) Tandon et al.[7] correlation

Fig. 3 - Influence of the convective heat transfer coefficient on the REFSIM program performance

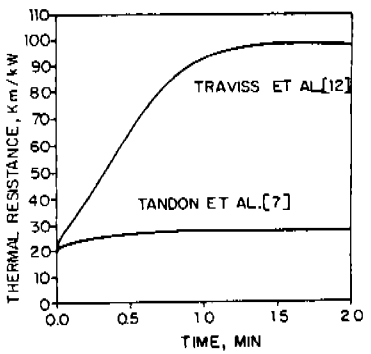

Fig. 4 - Comparison between the refrigerant side thermal resistances

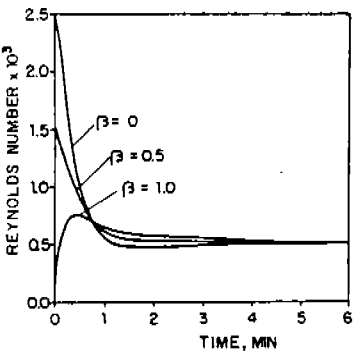

Fig. 5 - Reynolds number as a function of the adopted mass flow rate

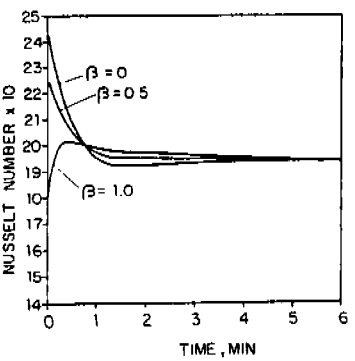

Fig. 6 - Nusselt number as a function of the adopted mass flow rate

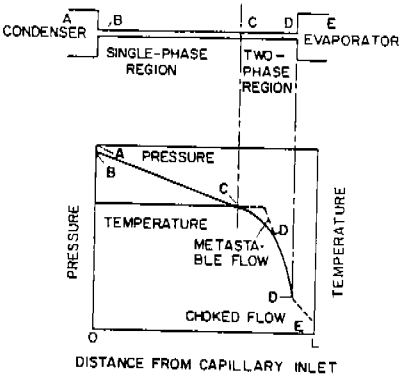

Fig. 7 - Pressure and temperature distribution along a capillary tube

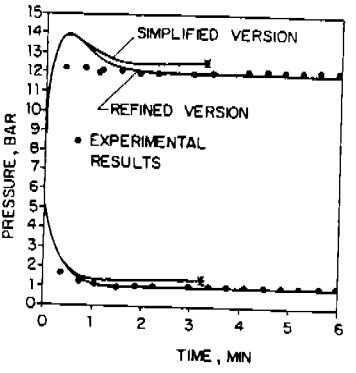

Fig. 8 - Simulated pressures in the system for different capillary tube models

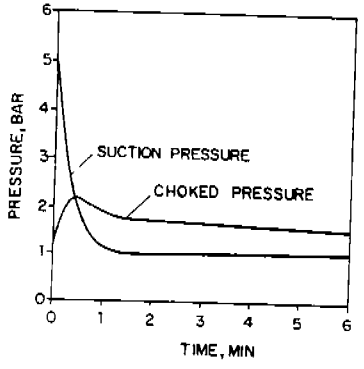

Fig. 9 - Simulated critical and suction pressures

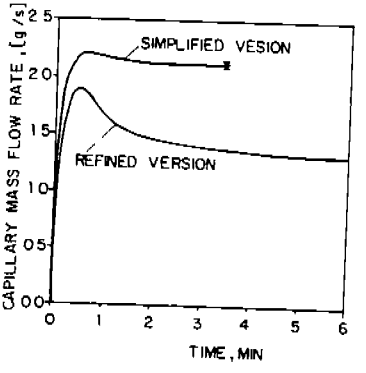

Fig. 10 - Simulated mass flow rates through the capillary tube

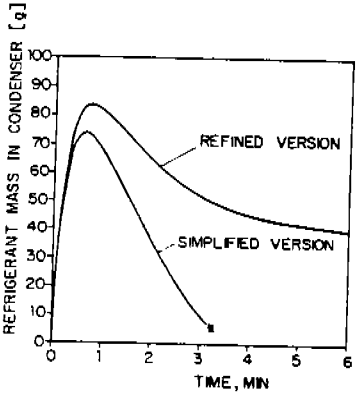

Fig. 11 - Simulated refrigerant mass in condenser for different capillary tube models

COMPUTING DESIGN OF HEAT PUMPS WITH THERMAL STORAGE

Václav Havelský

Department of Heat Engineering, Faculty of Mechanical Engineering of Slovak Technical University, 812 31 Bratislava, Czechoslovakia

ABSTRACT

This paper deals with the problems of designing heat pumps using atmospheric air as the external low temperature source of energy with the accumulation of thermal energy in a circuit of working fluid. The optimal dimensioning of heat pump systems with thermal storage by means of the computer simulation minimizes disadvantages occuring in heat pump systems without thermal storage and enables also reach of maximum available energy savings in dependence on the objective conditions of utilization of the designed heat pump.

INTRODUCTION

Residental heating load requirements, for a given building, increase with the decrease of outdoor temperature, and also depend on the building construction parameters. Therefore, covering all the thermal load requirements by heat pump systems, with atmospheric air as the external heat source, necessitates design of the heat pump heating capacity for the lowest expected temperature of the ourdoor air. Such a design has a lot of disadvantages: the oversizing of the whole system, the low annual utilization of the installed power input of the heat pump, an expensive control system /the heat pump is often operated at the lower end of the load range/ which results in high investment costs.

Improvements in the annual utilization of heat pumps with external air as the heat source can be achieved by sizing the heat pump capacity for an external temperature above the lowest expected temperature. This temperature determines the balance point, which is the point of intersection of the curve of heat pump heating capacity and heating load dependent on outdoor temperature.

For the outdoor temperatures above the balance point temperature, heat pump capacity is in excess of building load requirements. Below the balance point, the heat pump alone can no longer satisfy building head load requirements. The covering of all the heating load in this case can be achieved in combination with an auxiliary heating system or with the help of a heat accumulator installed in a working fluid circuit of a heat pump.

DESIGNING OF HEAT PUMP SYSTEMS WITH THERMAL STORAGE

Function of the Accumulation of the Heat in Working Fluid Circuit

The principle of the heat pump storage system with the accumulator of thermal energy in the working fluid circuit is shown in Fig.1, as is presented in [1]. There is a compressor heat pump circuit with the heat accumulator installed behind the condenser. For external temperatures above the balance point temperature the refrigerant, after passing through the condenser, is not immediately expanded to its evaporating pressure, but first flows through a heat exchanger inside the heat accumulator. The remaining condensation enthalpy is dependent on the existing external temperature, which is not required for heating, and is extracted from the working fluid in the accumulator.

If the external temperature is below the balance point temperature, the refrigerant flows from the condenser, via a three-way valve and an expansion valve, into the evaporator inside the accumulator extracting heat at store temperature. The usable temperature range of the accumulating temperature is limited by the condensing temperature which sets the upper limit, whilst the lower limit is determined by the balance point temperature.

Dimensioning of the Heat Pump with Thermal Storage

In the following we take into consideration a short-term storage, when the system is dimensioned according to the average daily temperature swing of the atmospheric air. The expected daily temperature course can be determined from the average maximum and minimum daily temperature by assumptions of the sinusoidal course between maximum and minimum temperatures.

The required heat capacity of the accumulator and the balance point temperature (which determines the installed heat pump capacity)

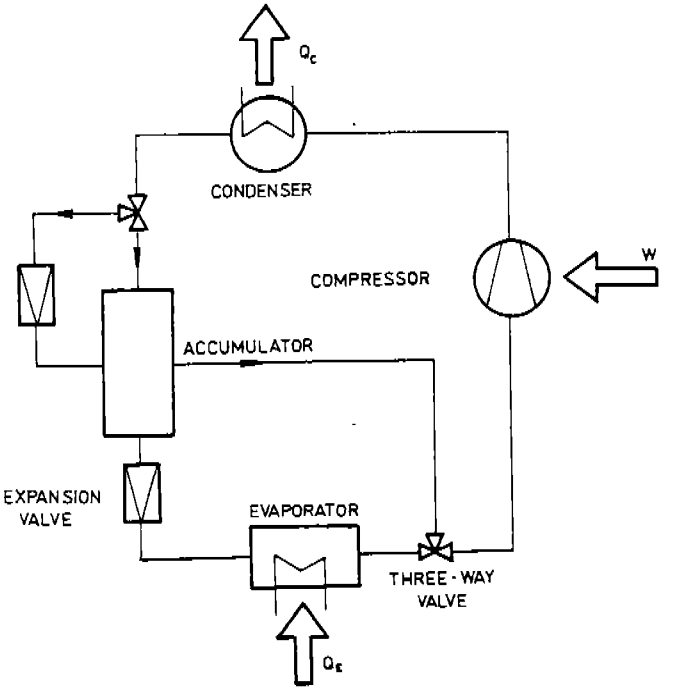

Fig.1: Heat pump system with the accumulator of thermal energy in the circuit of a working fluid schematic

can be calculated on the basis of the quantity of heat extracted from the accumulator into the working fluid for the discharge period /when the external temperature is below the balance point temperature/ and of the quantity of heat flowing into the accumulator from the working fluid for the charge period /when the external temperature is higer than the balance point temperature/.

The simple method for the determination of the mentioned quantities of heat is their calculation from the predicted coefficient of performance of the particular heat pump system by the method presented in [2]. For the determination of the length and diameter of evaporating and condensing tube in heat accumulator it is necessary to use the computer program to determine the thermophysical, properties of working fluids.

COMPUTER SIMULATION

Simulation Model

A simulation model has been developed so that, in a charge period, the designed system works with constant maximum power input and in a discharge period, the system works with a power input corresponding to the thermal load requirements dependent on the temperature of outdoor air.

The necessary input parameters for the corresponding computer program are:

1. Maximum heat flow rate from condenser $\dot{Q}_{c,max}$.
2. The temperature of working fluid in the condenser t_c.
3. The lowest expected temperature of outdoor air $t_{e,min}$, calculated value.
4. The internal /room/ temperature t_i.
5. The final /maximum/ accumulating temperature t_{af}.
6. The daily temperature time behaviour determined from average maximum t_{max} and minimum t_{min} daily temperatures.
7. The efficiency of the electric motor of electrically driven heat pumps η_e.
8. The mechanical efficiency of heat pump η_m.

The output values from the computer program are:

1. The balance point temperature t_{bp}.
2. The heat capacity of the acumulator C_a and corresponding size of evaporating and condensing tubes for heat accumulation to water.
3. The initial /minimum/ accumulating temperature t_{ai}.
4. The installed heat pump power input P.
5. The energy requirements of the heat pump with thermal storage E_a.
6. The energy requirements of the heat pump without thermal storage E.

The dependence of the accumulator heat capacity C_a and the installed power input P on the value of $\dot{Q}_{c,max}$ is shown in Fig.2 for the working fluids R 11, R 12 and R 22 for the constant input parameters t_c = 55 °C, $t_{e,min}$ = - 12 °C, t_i = 18 °C, t_{af} = 45 °C, t_{max} = 0,3 °C and t_{min} = - 4,9 °C /for Bratislava in Czechoslovakia in January/, η_e = 0,9 and η_m = 0,9.

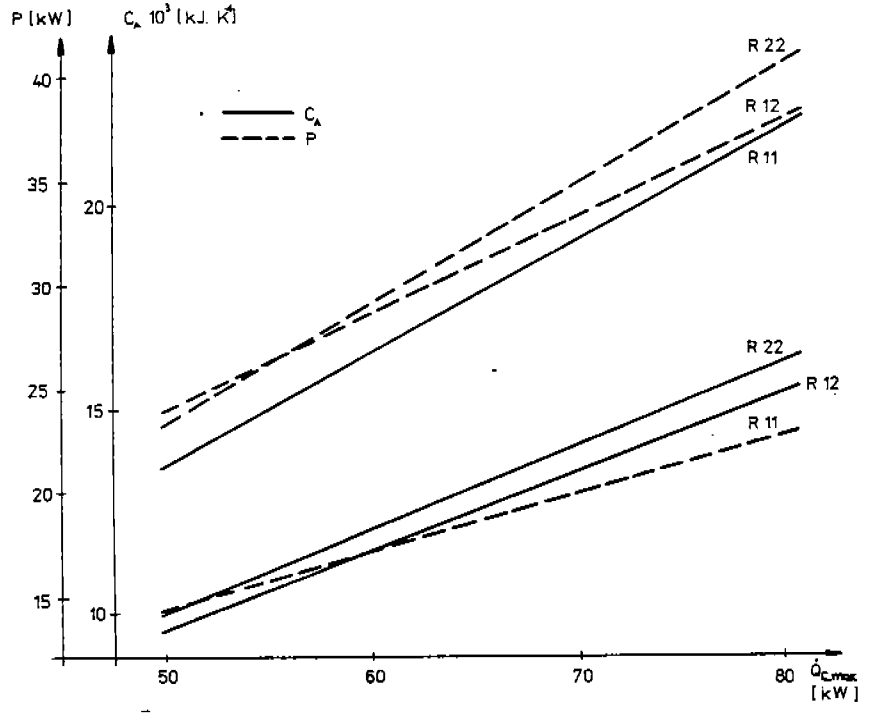

Fig.2. Accumulator heat capacity C_a and installed power input P vs. maximum heat pump capacity $\dot{Q}_{c,max}$ for different working fluids

The dependence of C_a on the value of t_{af}/t_c for $\dot{Q}_{c,max}$ = 50 kW and other constant input parameters as in Fig.2 is shown in Fig.3 for working fluids R 11, R 12 and R 22.

The dependence in Fig.2 shows, that necessary values of the installed power input P and the accumulator heat capacity C_a are very different in dependence of the aplicated working fluid for the constant value of $\dot{Q}_{c,max}$.

The dependence in Fig.3 shows, that with the increase of the maximum accumulating temperature t_{af} towards the condensing temperature t_c the value of the accumulator heat capacity C_a decreases considerably for the all working fluids. Then the weight and overall dimensions of the accumulator also considerably decrease. The other output values from the computer program t_{bp}, t_{ai}, E_a, E change only negligibly, the necessary installed power input P shows practically no change.

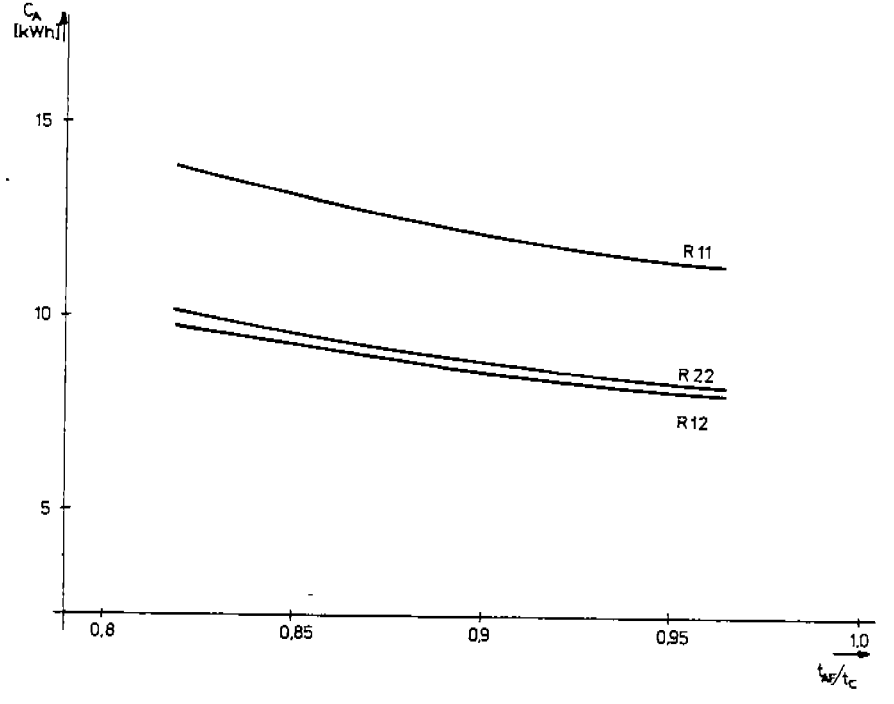

Fig.3: Accumulator heat capacity C_a vs. t_{af} / t_c for $\dot{Q}_{c,max}$ = 50 kW and different working fluids

Energy Savings

Calculation of the energy savings predicted by this simulation model assumes, that the compared heat pump without thermal storage works at temperatures above the balance point temperature with a power input corresponding to the thermal load requirements dependent on the temperature of outdoor air and the thermal load requirements at temperatures below the balance point are substitute by supplemental resistance heat.

The dependence of the energy requirements of the heat pump with thermal storage E_a and the energy requirements without thermal storage E for working fluids R 11, R 12 and R 22 and other constant input parameters as in Fig.2 on the value of $\dot{Q}_{c,max}$ is shown in Fig.4.

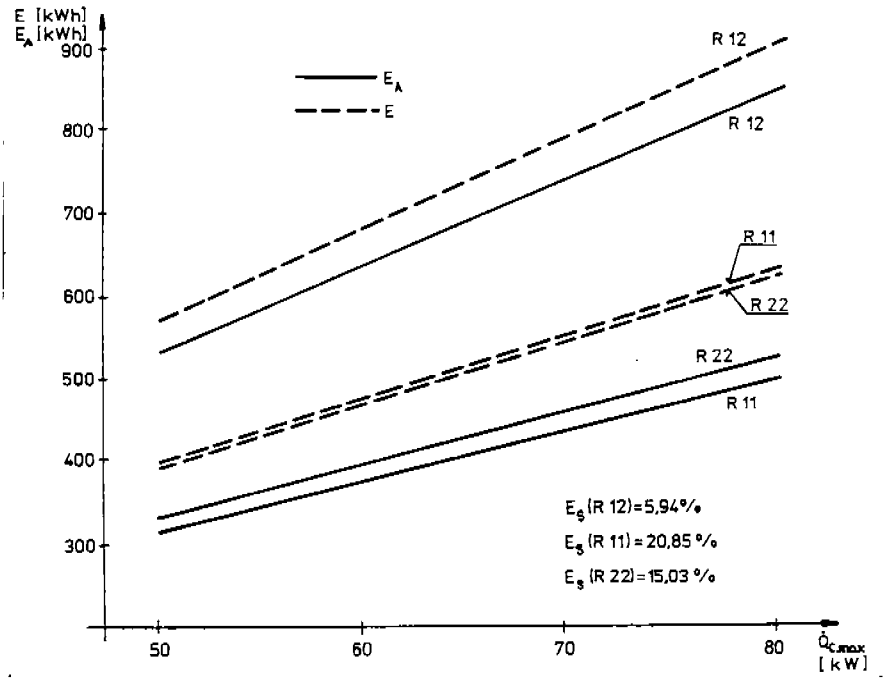

Fig.4: Energy requirements and energy savings vs. maximum heat pump capacity $\dot{Q}_{C,max}$ for different working fluids

The dependence in Fig.4 shows various values of energy requirements E_a and E at constant value of $\dot{Q}_{C,max}$ for different working fluids. There are also numerically illustrated the corresponding energy savings E_s ($E_s = E - E_a$), which are in percentage for the individual working fluid independent on the value of $\dot{Q}_{C,max}$.

CONCLUSIONS

Results from the computer simulation illustrated in Fig.2, 3 and 4 show, that the values of accumulator heat capacity, requied installed power input and energy savings in comparison with the heat pump without thermal storage depend considerably on the aplicated working fluid in

a circuit of the heat pump. It is also shown, that the increase of the maximum accumulating temperature towards the condensing temperature influences on decrease of the accumulator heat capacity without change of the requied installed power input of the heat pump.

The fact that when the temperature lift between condenser and evaporator is reduced, the actual value of coefficient of performance increases only slightly, must also be taken into consideration. The reason is that the actual compression work remains finite and it is ultimately due to almost entirely irreversible losses in the evaporator and condenser, as is shown in [3]. The decrease of the temperature lift between condensing and evaporating temperatures influences also the decrease of the efficiency of motor drive and consequently decreases the actual value of the coefficient of performance of the whole system.

The optimal design of heat pump systems with thermal storage, using computer simulation, can only be done when the objective conditions of utilization of the designed heat pump are taken into consideration. Then it will be possible to minimize the disadvantages occuring in heat pump systems without thermal storage and reach of the maximum available energy savings.

A series of experiments should be carried out with various heat pump systems with different working fluids to improve the methods of their optimal design.

REFERENCES

1. Cube,H.L., Steimle,F.:Heat Pump Technology. Butterworths (1981)
2. Mečárik,K., Havelský,V., Fúri,B.: Tepelné čerpadlá (Heat Pumps). Alfa/SNTL, Bratislava (1988)
3. Soumerai,H.: Predicting heat pump performance by thermodynamic generalizations of fluid flow and heat transfer data. Int.J.Refrig. 9, 113÷120 (1986)